Tropomyosin's Periods Are Quasi-Equivalent for Actin Binding but Have Specific Regulatory Functions†

Abhishek Singh‡,§,|| and Sarah E. Hitchcock-DeGregori*,‡

Department of Neuroscience and Cell Biology, Robert Wood Johnson Medical School, 675 Hoes Lane, Piscataway, New Jersey 08854, MD/PhD Program, Robert Wood Johnson Medical School, Piscataway, New Jersey 08854, and Joint Graduate Program in Biochemistry and Molecular Biology, UMDNJ-Graduate School of Biomedical Sciences and Rutgers University, Piscatway, New Jersey 08854

Received August 6, 2007; Revised Manuscript Received September 19, 2007

ABSTRACT: Tropomyosin is a coiled coil that associates N-terminus to C-terminus to form a continuous strand along both sides of the actin filament and regulates its function. One long, high molecular weight tropomyosin molecule spans the length of seven actin subunits. In these forms there is a 7-fold periodicity in noninterface residues that have been proposed to correspond to seven quasi-equivalent actin binding sites. Interruption of the stable, canonical coiled coil by residues that destabilize the interhelical interface, such as Ala clusters, is required for actin binding. Previous studies have shown that the N-terminal half of period 5 (residues 165−188) is critical for actin binding and regulatory function and that both the surface "consensus" residues and the embedded, destabilizing Ala cluster are required for function. In the present work we test the hypothesis of quasi-equivalence of tropomyosin's periodic sites by replacing the proposed binding sites by substituting the crucial period 5 region with regions of period 1 or 2. Replacement mutants were designed to test the importance of the coincidence of the consensus residues and a destabilizing interface. The results show that generic (interface instability) and specific periodic surface residues are essential for function and that the periods tested (periods 1, 2, and 5) are quasi-equivalent for actin binding. However, regulatory functions are period-specific: periods 1 and 5 for binding to actin in the force-producing state and period 5 for Ca^{2+}-dependent regulation with troponin.

Tropomyosin is a coiled coil that associates N-terminus to C-terminus to form a continuous strand following the actin filament helix, one strand on each side of the filament (*1*, *2*). Long-standing biochemical and biophysical research has come together with more recent cellular and genetic experiments to show that tropomyosin is a major cellular regulator of actin filament stability and binding of other proteins that modulate its function (*3*). In striated muscles, tropomyosin is known for its role in transmitting the Ca^{2+} signal that binds to troponin C along the filament and for making activation of the filament by myosin cooperative (*1*, *2*). From genetic and cellular studies we know that tropomyosin is involved in determining cell shape, intracellular vesicle movement, and cytokinesis. Underlying all these activities is the ability of tropomyosin to bind to actin.

Analyses of the tropomyosin sequence, from the time it was first determined, revealed periodicities in noninterface positions postulated to be seven quasi-equivalent actin binding sites along the length of one high molecular weight (HMW),[1] 284-residue tropomyosin (*4*−*6*). Figure 1 illustrates in striated muscle α-tropomyosin the 7-fold structural repeat that Phillips identified in the exposed positions of the helix, referred to here as "consensus residues" or a "consensus repeat" (Figure 1, in cyan; *6*, personal communication). The significance of the repeats may be inferred from the clustering of disease-causing mutations in these regions. McLachlan and Stewart (*5*, *7*) also noted a roughly periodic distribution of small nonpolar amino acids at the coiled coil interface, such as Ala (magenta in Figure 1), that would allow flexibility and bending of the tropomyosin supercoil on the actin filament helix. This idea is supported by the presence of bends in the coiled coil at the sites of "Ala clusters" and other noncanonical regions in the structure (*8*−*12*).

In previous work we showed that the flexibility or instability allowed by the interface Ala clusters is required for tropomyosin to bind actin (*13*, *14*) and that the specific surface "consensus" residues are crucial when colocalized with a poorly packed, unstable interface. We have proposed that there is a dual requirement for a specific recognition site on the surface and an unstable or flexible interface for a particular region of tropomyosin to bind to actin (*14*). These results, and others, support our general proposal that interac-

† This research was supported by NIH Grant RO1-36326 to S.E.H.-D. and an NIH Interdisciplinary Workforce Training Grant Fellowship to A.S.

* To whom correspondence should be addressed. Phone: (732) 235-5236. Fax: (732) 235-4029. E-mail: hitchcoc@umdnj.edu, singha2@umdnj.edu.

‡ Department of Neuroscience and Cell Biology, Robert Wood Johnson Medical School.

§ MD/PhD Program, Robert Wood Johnson Medical School.

|| UMDNJ-Graduate School of Biomedical Sciences and Rutgers University.

[1] Abbreviations: CD, circular dichroism; DTT, dithiothreitol; HMW, high molecular weight (tropomyosins); PIA, pyrene iodoacetamide; SDS−PAGE, sodium dodecyl sulfate−polyacrylamide gel electrophoresis; S1, myosin subfragment 1; TM, tropomyosin; TnT, troponin T.

10.1021/bi701570b CCC: $37.00
Published on Web 12/04/2007

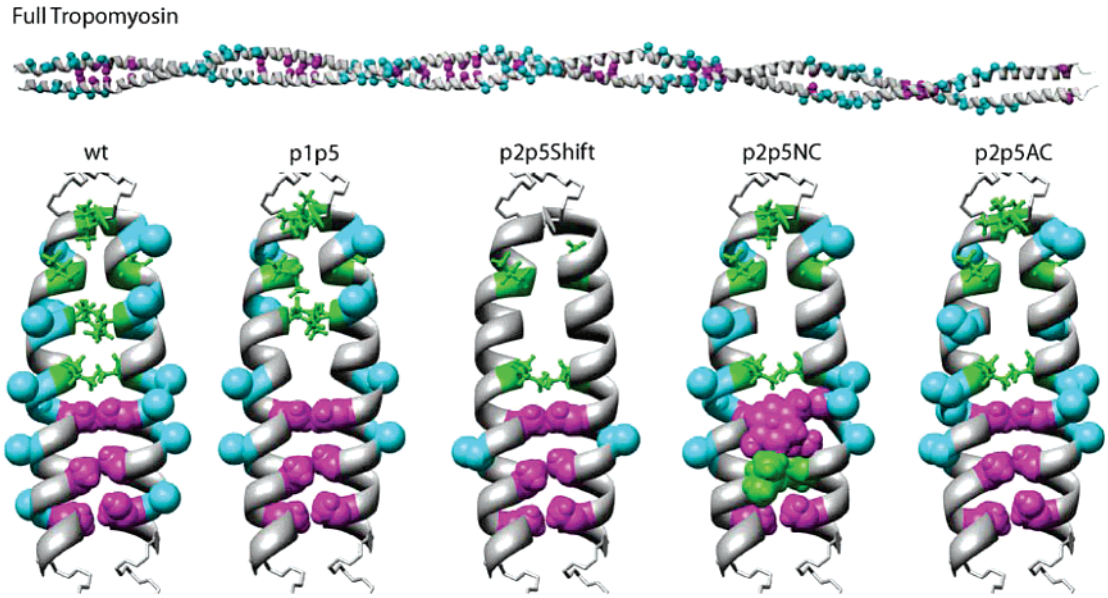

FIGURE 1: Structure of striated muscle α-tropomyosin. The side chains of the alanine clusters (magenta) and consensus actin binding sites (*6*; cyan) are illustrated on a ribbon model of the 7 Å structure (*39*). Below, residues 165−188 (part of period 5, encoded by exon 5) are enlarged with the side chains of interface Ala residues (magenta, space filling), canonical interface residues (green, sticks), and consensus residues (cyan, space filling with C_β shown). The colors used are the same as in Table 1.

tion of coiled coils with target molecules requires a flexible, less stable coiled coil at the binding site (*15*). Similarly, intrinsically unstructured regions in globular proteins are involved in functional interactions and fold upon binding to a target (*16*).

For period 5 to be a productive actin binding site requires the coupling of sequence specificity and a poorly packed interface (*14*). Can this be generalized to the other periodic repeats? In the present work we test the hypothesis of quasi-equivalence of the proposed binding sites: can one consensus site take the place of another? We have addressed this question in the context of the N-terminal half of period 5 (residues 165−188) of striated muscle α-tropomyosin since, unlike most other periods, deletion or replacement with the GCN4 leucine zipper leads to loss of tropomyosin's actin affinity and regulatory function (*17*, *18*). In contrast, when the consensus sites in period 2 (residues 47−60), period 3 (residues 89−102), or the C-terminal half of period 5 of striated α-tropomyosin (residues 189−213, containing the first two consensus residues of the sixth consensus site encoded by exon 6b) were replaced with the GCN4 sequence, all three retained the ability to bind actin (*18*, *19*). The loss of affinity exhibited bipolarity: the affinity of tropomyosins lacking single periods is in the following order (least effect to greatest effect): $2 > 3 \approx 4 \approx 6 \gg 5$ (*18*). Are the differences because of sequence or placement in the molecule?

To address these questions, we replaced the fifth consensus binding site (within residues 165−188) of striated muscle α-tropomyosin with corresponding sequences from period 1 or period 2. The results reported here suggest that the actin binding sites are quasi-equivalent. However, for maximal function there must be a region of instability within the consensus site. The results also suggest that period 5 is specially designed for actin binding and its role in Ca^{2+}-dependent regulation with troponin. We conclude from this and previous work that the interaction of a coiled coil motif with a target molecule requires coincident regions of lower stability that provide the molecular flexibility necessary to interact with the target, but that not all periodic repeats are designed for maximal actin affinity.

MATERIALS AND METHODS

Mutant Construction. Mutations were made in a rat striated muscle α-tropomyosin cDNA, gift of Dr. Bernardo Nadal-Ginard (*20*), cloned in pET11d (*21*) for expression in *Escherichia coli*. The mutations to replace the nucleotides encoding amino acid residues 165−188 were made using two-stage PCR as previously described (*13*, *22*) with the oligonucleotides below and their reverse complements. To facilitate incorporation of the mutations, aside from p1p5, the mutations were introduced in two or three stages with overlapping oligonucleotides, each encoding 12 or 8 mutant amino acids, respectively. We utilized codon optimization (lower case) to decrease the chance for annealing of the oligonucleotides to the wild-type sequence (lower case). All oligonucleotides were synthesized and PAGE purified by Integrated DNA Technologies (Skokie, IL).

p1p5:

5′-GACCGAAAGTATGAGGAgATCAAGAAGAAG-ATGCAGATGCTGAAGCTTGACAAAGAGAACG-CCTTGGATCGAGCAGAGCAGGCCGAGGCTaAA-TGTGCGGAGCTTG-3′.

p2p5Shift part 1:

5′-ACCGAAAGTATGAAGAgATTAAAAAAA-AAATGCAAATGCTGAAACTGGATAAaGAGCG-TGCGGAGGAGAGG-3′.

p2p5Shift part 2:

5′-CAAATGCTGAAACTGGATAAAgAAAAT-GCGCTGGATCGCGCGGAACAGGCGGAAGC-GaAATGTGCGGAGCTTG-3′.

p2p5AC part 1:

5′-GACCGAAAGTATGAAGAgCTGCAgAAaAAA-CTgAAGGGtACcGAAGATGAAcTGGAGCGTGC-GGAGGAGAG-3′.

p2p5AC part 2:

5′-gAAGGGtACcGAAGATGAAcTGGAtAAA-gcgTCgGAaGCggcgAAAGATtcgCAGGAaaAAT-GTGCGGAGCTTG-3′.

p2p5NC part 2:

There was only one set of oligonucleotides required for this mutant because we introduced the mutation (YLA) in place of the AAA of the p2p5AC mutation.

5′-GAAGATGAAcTGGAtAAAtatTCgGAaG-CgctgAAAGATgcgCAGGAaaAATGTGCGGAG-3′.

The presence of the mutations was verified by DNA sequencing of the entire cDNA by the DNA Core Facility at UMDNJ-Robert Wood Johnson Medical School.

General recombinant DNA techniques were performed as recommended by the supplier.

Protein Purification. Recombinant tropomyosins were overexpressed in *E. coli* BL21 (DE3) cells (*21*) using the autoinduction method (*23*). The proteins were purified as previously described (*24*, *25*) by heat denaturation following extraction, ammonium sulfate fractionation, and conventional chromatography in DE52 cellulose and hydroxylapatite.

Actin was purified from acetone powder of pectoral chicken skeletal muscle actin (*26*). Troponin was purified from chicken pectoral muscle (*27*). The recombinant fragment of human cardiac TnT_{70-170} used in all of the binding experiments was prepared as previously described (*28*). Myosin and myosin S1 were a generous gift from Dr. Donald Winkelmann (Department of Pathology, Robert Wood Johnson Medical School).

The tropomyosin and actin concentrations were determined by measuring the difference spectra in 6 M guanidine−HCl between pH 12 and pH 6.0 (*29*) and calculating the concentration using extinction coefficients of 2480 M^{-1} cm^{-1} for tyrosine (*30*) and 830 M^{-1} cm^{-1} for tryptophan (*31*). The concentrations of myosin, papain-digested myosin S1, and troponin were determined spectrophotometrically with extinction coefficients of 0.53, 0.83 and 0.45, respectively, at 280 nm (0.1%). The concentration of the $cTnT_{70-170}$ fragment was determined by the biuret assay.

Circular Dichroism Thermal Denaturation and Fluorescence Measurements. Thermal stability measurements were made by following the ellipticity of tropomyosin at 0.1 mg/mL at 222 nm as a function of temperature in 0.5 M NaCl, 10 mM sodium phosphate (pH 7.5), 1 mM EDTA, and 0.5 mM DTT (unless otherwise noted) in an Aviv model 215 spectropolarimeter with a total fluorescence attachment as previously described (*32*).

The tropomyosins were modified at Cys190 with pyrene iodoacetamide (PIA) in the presence of guanidine−HCl following the protocol of Ishii and Lehrer (*33*). The bound pyrene was determined to be 80−110% on the basis of the extinction coefficient of bound pyrene iodoacetamide and the free sulfhydryl determined using $[NbS]_2$ (*30*).

Fluorescence spectra were obtained on some of the mutants using a PTI fluorimeter with a water bath (Lawrenceville, NJ) with an excitation at 340 nm and a scan from 360 to 560 nm, monitoring the monomer peaks at 385 and 405 nm and the excimer peak at 480 nm.

Actin Binding Assays. The affinity of tropomyosin for filamentous actin was measured by cosedimentation (*34*). Tropomyosin (0.1−10 μM, depending on the tropomyosin) and 0.12−12 μM troponin T_{70-170} (*28*) were combined with 5 μM actin and sedimented in a Beckman model TL-100 ultracentrifuge in a TLA-100 rotor at 60 000 rpm for 25 min at 20 °C in 200 mM NaCl, 10 mM Tris−HCl, pH 7.5, 2 mM $MgCl_2$, and 0.5 mM DTT (unless otherwise noted). The TnT_{70-170} fragment, which binds to the carboxyl terminus of tropomyosin (*28*), was added at a 1.2× molar excess to increase the affinity of unacetylated, recombinant striated muscle tropomyosin for actin. The pellets and supernatants were analyzed on 12% SDS−PAGE (*35*), stained with Coomassie Blue, and analyzed on a Molecular Dynamics model 300A computing densitometer. The free tropomyosin in the supernatants was calculated from standard curves for wild-type tropomyosin.

The apparent K_{app} of tropomyosin for F-actin and the Hill coefficient (α^H) were determined by fitting the experimental data to the following equation using SigmaPlot (Jandel Scientific, San Rafael, CA):

$$\upsilon = n[\mathrm{TM}]^{\alpha^H} {K_{app}}^{\alpha^H}/(1 + [\mathrm{TM}]^{\alpha^H} {K_{app}}^{\alpha^H})$$

where υ = fraction maximal TM binding to actin, n = maximal TM bound, and $[TM] = [TM]_{free}$. The TM:actin ratio was normalized to 1.0 by dividing the TM:actin ratio obtained from densitometry by the observed TM:actin maximal ratio at saturation.

Actomyosin MgATPase Assay. The actomyosin MgATPase was measured as a function of tropomyosin concentration using 2.4 μM F-actin, 0.6 μM myosin, 0−2 μM tropomyosin, 1 μM troponin in 40 mM NaCl, 5 mM imidazole (pH 7.0), 0.5 mM $MgCl_2$, 5 mM MgATP, 1 mM DTT, and 0.2 mM EGTA or 0.2 mM $CaCl_2$ as previously described (*34*). Assays were carried out at a final volume of 75 μL in a 96-well microtiter plate at 28 °C in a thermoequilibrated Molecular Devices ThermoMax microtiter plate reader. The reaction was initiated by addition of MgATP to a final concentration of 5 mM and terminated with the addition of 25 μL of 13.4% SDS, 0.12 M EDTA after 15 min. The amount of inorganic phosphate released was determined calorimetrically against a titrated amount of known inorganic phosphate (*36*). The plates were read in the microtiter plate reader with a 650 nm filter. Previous time courses have shown that the amount of inorganic phosphate released is linear over a time course of 15 min.

Myosin S1-Induced Tropomyosin Binding Assay. Actin (3 μM) and tropomyosin (1 or 2 μM where indicated) were mixed with myosin S1 (0 to 3.6 or 6 μM) in poor tropomyosin binding conditions (30 mM NaCl, 10 mM imidazole (pH 7.0), 0.5 mM $MgCl_2$, 1 mM DTT) (*37*, *38*). The mixture was incubated at room temperature for 2 h to ensure hydrolysis of residual ATP from F-actin and then centrifuged at 60 000 rpm and 20 °C for 25 min in a Beckman TL-100 ultracentrifuge in a TLA-100 rotor. The pellets were washed with assay buffer, then solubilized in actin extraction buffer (5 mM imidazole (pH 7.0), 0.1 mM $CaCl_2$, 0.1 mM ATP, 0.5 mM DTT) by sonication, and left overnight at 4 °C. The pellets were analyzed using SDS−PAGE as described above. The results were plotted as the S1:actin ratio (observed in the pellet) versus the total S1:actin molar ratio to determine the S1 saturation point (not shown) and as the TM:actin ratio (observed in the pellet) versus the total S1:actin molar ratio to determine the

Table 1: Tropomyosin Period 5 Mutants[a]

	d 165	e 166	f 167	g 168	a 169	b 170	c 171	d 172	e 173	f 174	g 175	a 176	b 177	c 178	d 179	e 180	f 181	g 182	a 183	b 184	c 185	d 186	e 187	f 188
Period 5 wt	V	A	R	K	L	V	I	I	E	S	D	L	E	R	A	E	E	R	A	E	L	S	E	G/S
Proposed Consensus Residues			K or R				NP		E				E or D	K or R			D or E				NP			
p1p5	I	K	K	K	M	Q	M	L	K	L	D	K	E	N	A	L	D	R	A	E	Q	A	E	A
p2p5AC	L	Q	K	K	L	K	G	T	E	D	E	L	D	K	A	S	E	A	A	K	D	S	Q	E
p2p5NC	L	Q	K	K	L	K	G	T	E	D	E	L	D	K	Y	S	E	A	L	K	D	A	Q	E
p2p5Shift	T	E	D	E	L	D	K	Y	S	E	A	L	K	D	A	Q	E	K	A	T	D	A	E	A
Exon 5-Zip	L	E	D	K	V	E	E	L	L	S	K	N	Y	H	L	K	N	E	V	A	Q	A	E	A

[a] The sequences of the mutated regions are shown. The blocked columns are the seven consensus residues in the b, c, and f positions, highlighted in cyan if they are maintained in the sequence. NP = nonpolar. Canonical interface residues in the a and d positions are in green. Destabilizing interface residues in the region of the Ala cluster are magenta. Models of the mutated regions are shown in Figure 1. The Exon 5-Zip sequences are fully described in ref *14*. Only Exon 5-Zip is shown. In Exon 5-Zip-AAS and Exon-5-Zip-QNQ, AAS and QNQ are in the Ala cluster positions of the wild-type and replace canonical residues in Exon 5-Zip. In Exon 5-Zip-Revert eleven residues were changed from the Exon 5-Zip to the wild-type period 5 residues: the Ala cluster AAS, the seven consensus residues of the period 5 wild-type, and K180, which was changed to the wild-type residue Glu.

cooperativity of binding. The TM binding data were fit to a modified version of the equation shown above to determine the curve midpoint:

$$v = [n[X]^{\alpha^H}K_{app}{}^{\alpha^H}/(1 + [X]^{\alpha^H}K_{app}{}^{\alpha^H})] + B$$

where v = TM:actin ratio in the pellet, [X] = total S1:actin molar ratio, and B = TM:actin ratio without S1. The S1:actin ratio necessary for half-maximal saturation of actin with TM is equal to $1/K$. Each TM−actin binding curve was normalized to 1.0 by dividing the observed TM:actin ratios at saturation by the maximal ratio ($n + B$) reported by SigmaPlot.

Molecular Modeling. Modeling was carried out using SYBYL (Tripos, Inc.). The mutations were introduced into the 7 Å structure (*39*; PDB entry 1C1G). The molecular graphics images were produced using the UCSF Chimera package from the Computer Graphics Laboratory, University of California, San Francisco (*40*), supported by NIH Grant P41 RR-01081.

RESULTS

Mutant Design. We tested the quasi-equivalence of tropomyosin's periodic sites based on the Phillips 1986 model (*6*, *41*, personal communication). He identified a 7-fold repeat of seven charged and nonpolar residues in noninterface b, c, and f positions of the heptapeptide repeat, which we refer to as "consensus" residues (Figure 1, Table 1). The repeats roughly correspond to the α-zones in McLachlan and Stewart's earlier reported 7-fold $39^1/_3$-residue periodicity of alternating α- and β-zones in a linear analysis of the sequence (*5*). Phillips, in contrast, took into account the azimuthal position of the side chains in the heptapeptide repeat of the helical coiled coil. Therefore, the Phillips repeats are multiples of seven residues, either 35 or 42 residues, with an average length of $39^1/_3$ residues. All mutations preserve the coiled coil heptapeptide repeat and are based on the axial and azimuthal positions of the residues within a given Phillips period.

We replaced the N-terminal region of period 5 (165−188) with regions of period 1 or 2 (Figure 1, Tables 1 and 2),

Table 2: Tropomyosin Period 5 Mutant Construction[a]

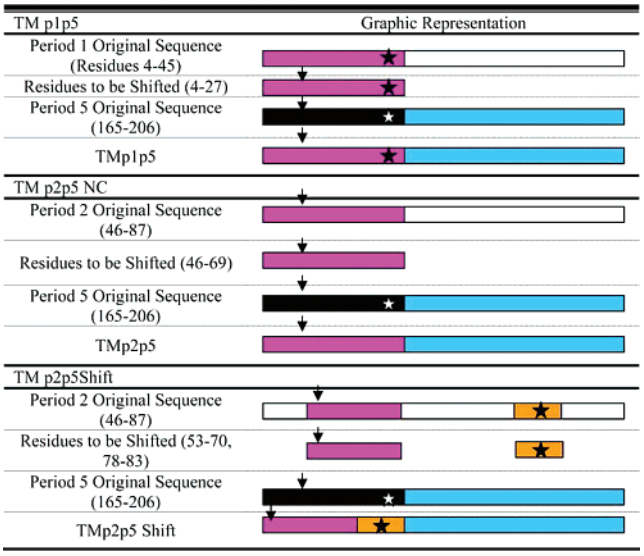

[a] Table of the period 5 replacement mutants. Residues in period 5 were replaced with residues from period 1 or period 2. The difference between the p2p5NC and p2p5AC (not in the table) mutants is that residues 179, 183, and 186 were changed to the wild-type Ala cluster in p2p5AC (see Table 1 for sequence comparison). The arrow indicates the position of the fourth consensus residue which is mislocated in p2p5Shift. The asterisk marks the middle of the Ala cluster.

regions that are expressed in striated muscle and HMW nonmuscle tropomyosin isoforms (*3*). Of the seven repeats, periods 1 and 5 are the most similar in sequence, and they are the only periods with an Ala cluster within a consensus site. To test the quasi-equivalence of period 1, we replaced residues 165−188 of period 5 with residues 4−27 from period 1 to make a tropomyosin we call p1p5 that has two period 1 sequences. This is a "direct" replacement where the position was based on the alignment of the periodic consensus repeat. In p1p5 the period 5 region retains the Ala cluster in the proper position and has four of seven consensus residues (Figure 1, Tables 1 and 2).

In period 2 the Ala cluster is C-terminal to the consensus site (Figure 1, Table 2). We made three mutants involving the replacement of period 5 with period 2 to assess the

contributions to quasi-equivalence of interface instability and the surface consensus residues. With direct replacement of period 5 with period 2, p2p5NC (no change, no cluster) based on the alignment of the consensus residues, there are five of seven consensus residues, but an incomplete Ala cluster (YLA; Figure 1, Tables 1 and 2). The p2p5AC (with Ala cluster) mutant contains the same sequence as p2p5NC, except AAS, the Ala cluster native to period 5, replaces YLA. To test the importance of proper positioning of the consensus residues in the presence of a destabilizing cluster, we made the p2p5Shift mutant where the Ala cluster was aligned but the consensus residues are misaligned and only one consensus residue is in the proper position. The mutations are in rat striated muscle α-tropomyosin cDNA (*20*) and were expressed in *E. coli*. The recombinant proteins were evaluated for actin affinity, regulatory function, and the effect of the mutations on local and global stability.

Functional Analysis: Actin Affinity. The ability to bind filamentous actin is a fundamental tropomyosin function. Since the sequence of period 1 is the most similar of the seven repeats to the period 5 sequence (*42*), it comes as no surprise that the p1p5 mutant binds with just a 2-fold decrease in actin affinity compared to the wild-type and lower cooperativity (Figure 2A, Table 3).

The actin affinity of the period 2 into period 5 mutants depends on the presence of consensus residues and a destabilizing Ala cluster (Figure 3A, Table 3). The p2p5Shift mutant that contains an Ala cluster with a misaligned consensus site did not bind actin. In contrast, when the consensus residues were properly aligned, with an Ala cluster introduced, as in p2p5AC, the binding was cooperative and saturable with just a 2-fold decrease in affinity compared to that of the wild-type. The p2p5NC mutant that contains the native period 2 interface residues YLA, a more stable interface than the Ala cluster, but less stable than a canonical LVL sequence, bound weaker than p1p5 and p2p5AC, but much better than the nonfunctional p2p5Shift mutant.

The results show that, in terms of actin affinity, period 1 and period 2 are quasi-equivalent to period 5. The coincident requirement for properly aligned surface consensus residues and an unstable interface agrees with our previous study of the requirements for restoration of actin binding ability to the mutants in which a GCN4 leucine zipper sequence replaced the period 5 sequence (Exon 5-Zip) (*14*). Nevertheless, since the mutants do not fully mimic wild-type tropomyosin, additional features must contribute to wild-type affinity and cooperativity. p2p5Shift and the Exon 5-Zip mutant with a restored Ala cluster (Exon 5-Zip-AAS) are similar in that three or fewer out of eighteen noninterface residues are in common with the wild-type. Neither binds to actin (Tables 1 and 3).

Functional Analysis: Myosin S1-Induced Binding of Tropomyosin to F-Actin in the Open, Force-Producing State. Tropomyosin bound to actin is in equilibrium between the closed and open force-producing states, according to the Geeves and Lehrer model (*43*−*45*). The binding of myosin heads to actin cooperatively shifts the equilibrium of the actin−tropomyosin filament from the closed state to the open state in which tropomyosin and myosin both bind to actin with higher affinity. In the fully activated, open state, myosin forms cross-bridges with actin and generates force. One way this function is manifested is by an increase in the affinity

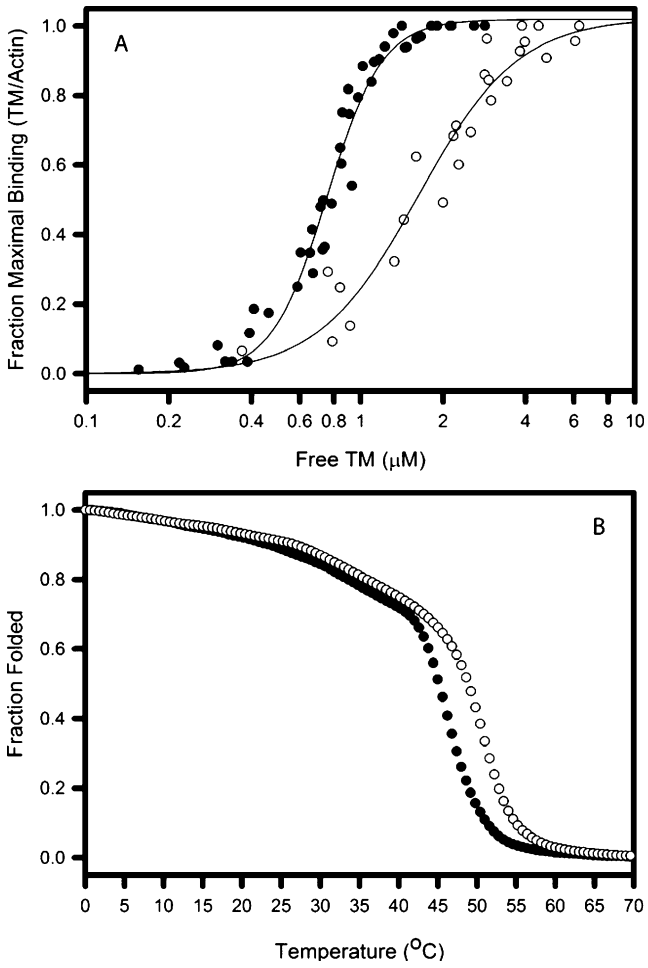

FIGURE 2: Effect of replacement of period 5 with period 1 on actin affinity and thermal stability. (A) Binding to filamentous actin. Tropomyosin (0.12−8 μM, depending on the tropomyosin) and 0.15−12 μM troponin T_{70-170} were combined with 5 μM actin and sedimented at 20 °C in 200 mM NaCl, 10 mM Tris−HCl (pH 7.5), 2 mM $MgCl_2$, and 0.5 mM DTT. The actin affinity was measured in the presence of a cardiac TnT_{70-170} fragment that binds to the C-terminus of striated muscle tropomyosin and increases the affinity of the unacetylated recombinant tropomyosin for actin (*28*). Stoichiometric binding of one tropomyosin per seven actins is represented by the 1.0 fraction of maximal binding. The apparent K_{app} values are reported in Table 3. (B) Fraction folded as measured by the relative ellipticity at 222 nm as a function of temperature. The tropomyosin concentration was 0.01 mg/mL. The T_M values are reported in Table 3. The fraction folded is relative to the mean residue ellipticity at 0 °C where the proteins were fully folded. Symbols: ●, wild-type; ○, p1p5.

of tropomyosin for actin by myosin S1 (*37*, *46*). Evidence for cooperativity is saturation of the actin filament with tropomyosin with fractional myosin S1 saturation (in the absence of ATP).

The cooperativity with which myosin S1 induces tropomyosin binding to actin correlates with actin affinity; tropomyosins that are unable to bind to actin do not bind with myosin S1 or bind with low cooperativity (*47*). The myosin S1-induced binding of the present tropomyosin mutants corroborates this generalization while giving new insight into the sequence and stability requirements for this regulatory function (Figure 4, Table 3). The p1p5 mutant binds with near wild-type S1/actin cooperativity (Figure 4A). Although the p2p5NC and p2p5AC mutants have actin affinity similar to that of p1p5 and bind actin with greater

Table 3: Actin Affinity and T_M from the Ellipticity at 222 nm of Tropomyosin Period 5 Mutants

tropomyosin	K_{app}[a] (10^6 M^{-1})	S1:actin molar ratio	CD T_M[b] (°C)
wild-type exon 5	1.32 ± 0.02	0.28 ± 0.03	46.3
p1p5	0.61 ± 0.03	0.34 ± 0.03	48.9
p2p5AC	0.77 ± 0.01	0.56 ± 0.04	43.6
p2p5NC	0.52 ± 0.01	0.68 ± 0.04	49.4
p2p5Shift	ND	ND	44.4
Exon 5-QNQ[c]	1.9 ± 0.07	0.25 ± 0.01	41.8
Exon 5-LVL[c]	ND	ND	56.4
Exon 5-Zip-Revert[c]	0.45 ± 0.02	0.35 ± 0.01	45.0
Exon 5-Zip-QNQ[c]	ND	0.46 ± 0.04	43.6
Exon 5-Zip-AAS[c]	ND	0.56 ± 0.03	45.0
Exon 5-Zip[c]	ND	ND	56.4

[a] The actin affinity and CD data have been previously published (*14*). The actin binding data were fit to the Hill equation, and K_{app} is that reported by SigmaPlot. [b] T_M is the point at which 50% of TM is unfolded. [c] The K_{app} and CD data have been published (*14*). K_{app} for the wild-type was 1.85×10^6 M^{-1}. ND means K_{app} was not measurable, less than 0.01×10^6 M^{-1}.

cooperativity, the myosin S1-induced binding is less cooperative, reaching saturation when the actin is saturated with myosin (Figure 4B). In contrast, myosin S1 did not induce actin binding of the p2p5Shift mutant, giving evidence for the importance of the period 2 consensus residues.

To further understand the effect of the non-native sequence on cooperative activation of the actin filament by myosin S1, we did the same analysis on a series of previously described period 5 (exon 5) mutants (Table 1) (*14*). The specific design of these mutants and their functional properties are described in detail elsewhere (*14*). In brief, the mutations were designed with two strategies. In the first, the hydrophobicity of the residues at the interface Ala cluster in wild-type period 5 (AAS; Table 1) was altered by introducing either a canonical, stabilizing LVL (Exon 5-LVL) or an Ala stability mimic QNQ (Exon 5-QNQ). In the second strategy, systematic mutations were made in interface and noninterface residues of a nonfunctional exon 5 GCN4 leucine zipper mutant (Exon 5-Zip; Table 1) and tested for recovery of function (*14*). In Exon 5-Zip-AAS and Exon 5-Zip-QNQ the canonical leucine zipper interface, LVL, was destabilized. In Exon 5-Zip-Revert the seven surface consensus residues as well as the AAS Ala cluster were substituted for the GCN4 leucine zipper sequence. Of the remaining 14 residues in the residue 165−188 region, 11 differ from those of the wild-type.

There is a requirement for both coiled coil interfacial instability and specific surface residues for myosin S1-induced binding of tropomyosin, as for binding to actin alone. The two mutants with canonical, LVL interfaces (Exon 5-LVL and Exon 5-Zip) did not saturate F-actin in either the cosedimentation assays or the presence of myosin S1 (Figure 4C,D, Table 3). In contrast, the cooperativity of the induced binding of the wild-type (AAS interface) was the same as with a QNQ interface (Exon 5-QNQ, Table 3, Figure 4C). Moreover, restoration of flexibility in the nonfunctional zipper mutants with a destabilizing cluster in the wild-type interface Ala positions, Exon 5-Zip-AAS and Exon 5-Zip-QNQ, did allow myosin S1 to induce tropomyosin to bind in the open state, but the binding was not cooperative, as indicated by the 1:1 S1:actin ratio required for saturation (Figure 4D). Restoration of the consensus actin binding

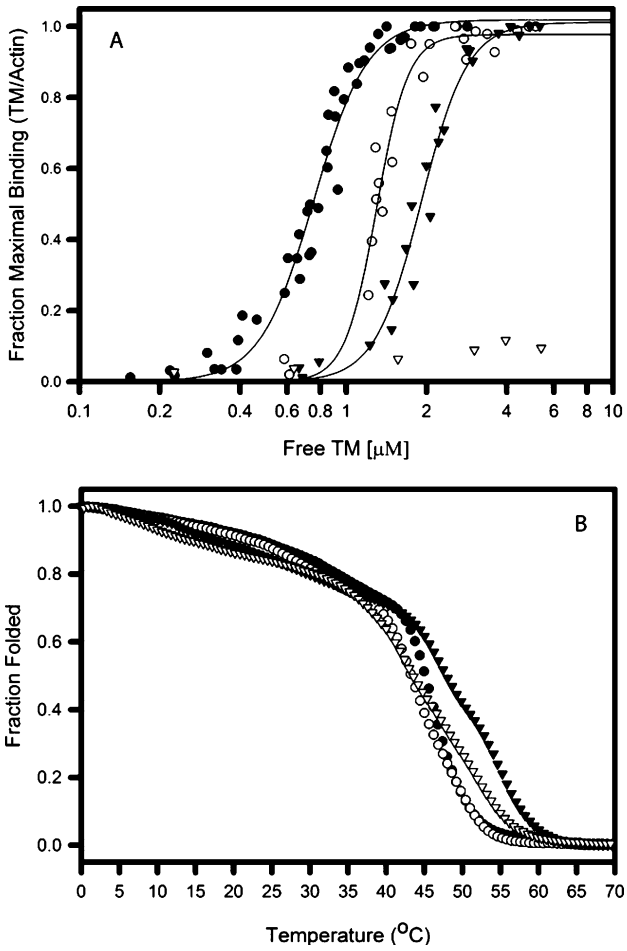

FIGURE 3: Effect of replacement of period 5 with variations of period 2 on actin affinity and thermal stability. (A) Binding to filamentous actin. Tropomyosin (0.12−8 μM, depending on the tropomyosin) and 0.15−12 μM troponin T_{70-170} (*28*) were combined with 5 μM actin and sedimented as in Figure 2. The apparent K_{app} values are reported in Table 3. (B) Fraction folded as measured by the relative ellipticity at 222 nm as a function of temperature. The tropomyosin concentration was 0.01 mg/mL. The T_M values are reported in Table 3. The fraction folded is relative to the mean residue ellipticity at 0 °C where the proteins were fully folded. Symbols: ●, wild-type; ○, p2p5AC; ▼, p2p5NC; ▽, p2p5Shift.

residues coupled with native destabilization (AAS) in the Exon 5-Zip-Revert allowed near wild-type cooperativity of S1-induced binding, as seen with p1p5.

The data suggest that flexibility and a consensus sequence are both important for S1-induced binding, as they are for binding to actin alone. However, while mutants with period 1 or 2 substituted for period 5 have equivalent actin affinities (in the presence of TnT), they differ in their binding to actin in the open state (with myosin S1, in the absence of troponin T). The period 5 consensus residues are critical since the Exon 5-Zip mutant with the consensus residues and Ala cluster (Exon 5-Zip-Revert) is similar to both the wild-type and the p1p5 mutant. In contrast, the cooperativity of the p2p5 mutants (with or without an Ala cluster) is similar to that of the destabilized Exon 5-Zip mutants lacking the consensus sequence that do not bind actin alone in the absence of myosin S1. The results suggest that period 1 and period 5, but not period 2, are quasi-equivalent for myosin S1 switching the actin filament to the open state. We emphasize, however, that these experiments do not offer

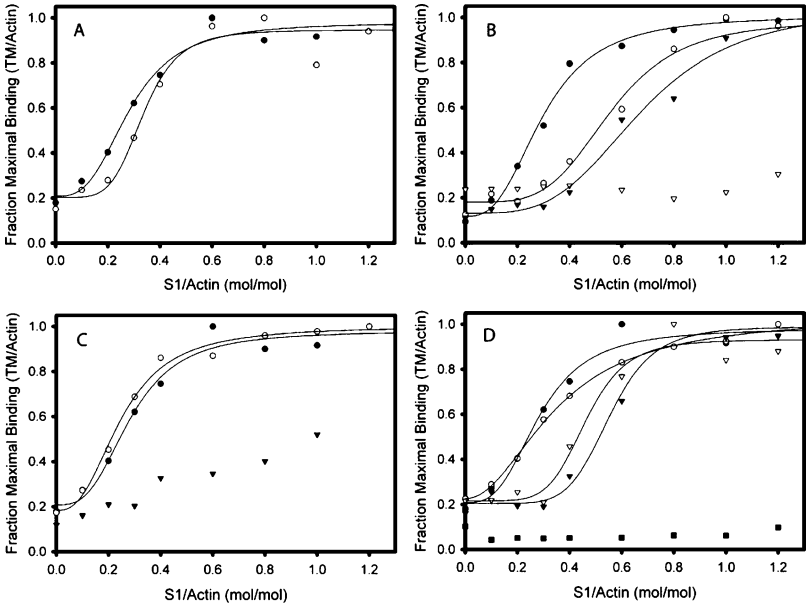

FIGURE 4: Myosin S1-induced binding of tropomyosin mutants to actin. Binding of TM (1 μM) and S1 to actin (3 μM) were measured as a function of S1 concentration (0−4.2 μM) in 30 mM NaCl, 10 mM imidazole (pH 7.0), 0.5 mM $MgCl_2$, 1 mM DTT. Data are from representative experiments. The observed TM:actin ratios from densitometry of SDS−polyacrylamide gels of the pellets were normalized to the ratio obtained with TM at saturation and plotted versus the total myosin S1:actin ratio (myosin saturates at a 1:1 ratio with actin). (A) Period 1 to period 5 replacement. Symbols: ●, wild-type; ○, p1p5. (B) Period 2 to period 5 replacement. Symbols: ●, wild-type; ○, p2p5AC; ▼, p2p5NC; ▽, p2p5Shift. (C) Period 5 stability and leucine zipper mutants (described in ref *14*). Symbols: ●, wild-type; ○, Exon 5-QNQ; ▼, Exon 5-LVL. At a higher Exon 5-LVL concentration (2 μM) S1 was able to induce saturable binding (data not shown). (D) Period 5 non-native mutants (described in ref *11*). Symbols: ●, wild-type; ○, Exon 5-Zip-Revert; ▼, Exon 5-Zip-AAS; ▽, Exon 5-Zip-QNQ; ■, Exon 5-Zip.

insight into the mechanism of cooperativity, that is, the sequential order of events.

Functional Analysis: Ca^{2+}-Dependent Regulation of the Actomyosin ATPase with Troponin. Tropomyosin, together with troponin, is required for Ca^{2+}-dependent regulation of the actomyosin ATPase (*1*). In the absence of Ca^{2+}, inhibition of in vitro actomyosin ATPase activity mimics "relaxation" and is a measure of the ability of tropomyosin to occupy the blocked state of the three-state model (*45*). The binding site for the globular head region of troponin on tropomyosin includes the residue 165−188 region (reviewed in ref *2*).

To determine the importance of sequence in Ca^{2+} regulation of the actomyosin ATPase, we selected three mutants that bind well to actin and are the most similar to the wild-type in the myosin S1 binding analysis. The p1p5, Exon 5-QNQ, and Exon 5-Zip-Revert mutants have similar local stability, but different noninterface residues. The mutants differ in their ability to switch the regulated thin filament from the closed or open state to the blocked state (Figure 5). The major difference between the mutants is in their ability to fully inhibit the actomyosin ATPase in the absence of Ca^{2+}. Exon 5-QNQ inhibited as well as the wild-type, while Exon 5-Zip-Revert required a ~2-fold higher concentration for 50% maximal inhibition, consistent with its weaker actin affinity (Table 3; *14*). The p1p5 mutant was ~6-fold less effective at inhibiting the regulated actomyosin ATPase in the absence of Ca^{2+} than the wild-type, poorer than would be expected with an actin affinity only 2-fold weaker than that of the wild-type (Table 3). Inhibition was not maximal even at 2 μM, at which the actin should be saturated with tropomyosin−troponin. We anticipate that there would be full inhibition at a higher tropomyosin concentration. Ca^{2+} relieved inhibition, though there was residual concentration-dependent inhibition, often observed in the conditions of the assay, except with p1p5.

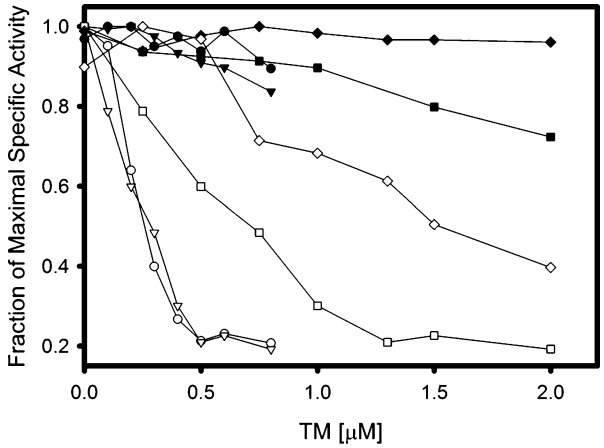

FIGURE 5: Actomyosin ATPase regulation of selected tropomyosin mutants with troponin. The ATPase of actin (2.4 μM), myosin (0.6 μM), Tn (1 μM), and TM (0−2 μM depending on the TM) was measured at 28 °C in 40 mM NaCl, 5 mM imidazole (pH 7.0), 5 mM $MgCl_2$, 0.5 mM DTT, and either 0.2 mM $CaCl_2$ or 0.2 mM EGTA. The reaction was initiated by addition of 5 mM MgATP. The results are from one representative experiment. Specific activity was normalized to the value in the absence of TM. Filled symbols are in the presence of Ca^{2+} and clear symbols in the presence of EGTA. Symbols: ●, ○, wild-type; ▼, ▽, Exon 5-QNQ; ■, □, Exon 5-Zip-Revert; ◆, ◇, p1p5.

The poor inhibition in the absence of Ca^{2+} and the full activity in the presence of Ca^{2+} suggest that troponin binding by p1p5 is impaired and that the period 5 consensus residues are part of the Ca^{2+}-sensitive troponin binding site on tropomyosin. The region of tropomyosin C-terminal to the period 5 mutations, encoded by exon 6 and including Cys 190, has been shown in previous work to be sensitive to

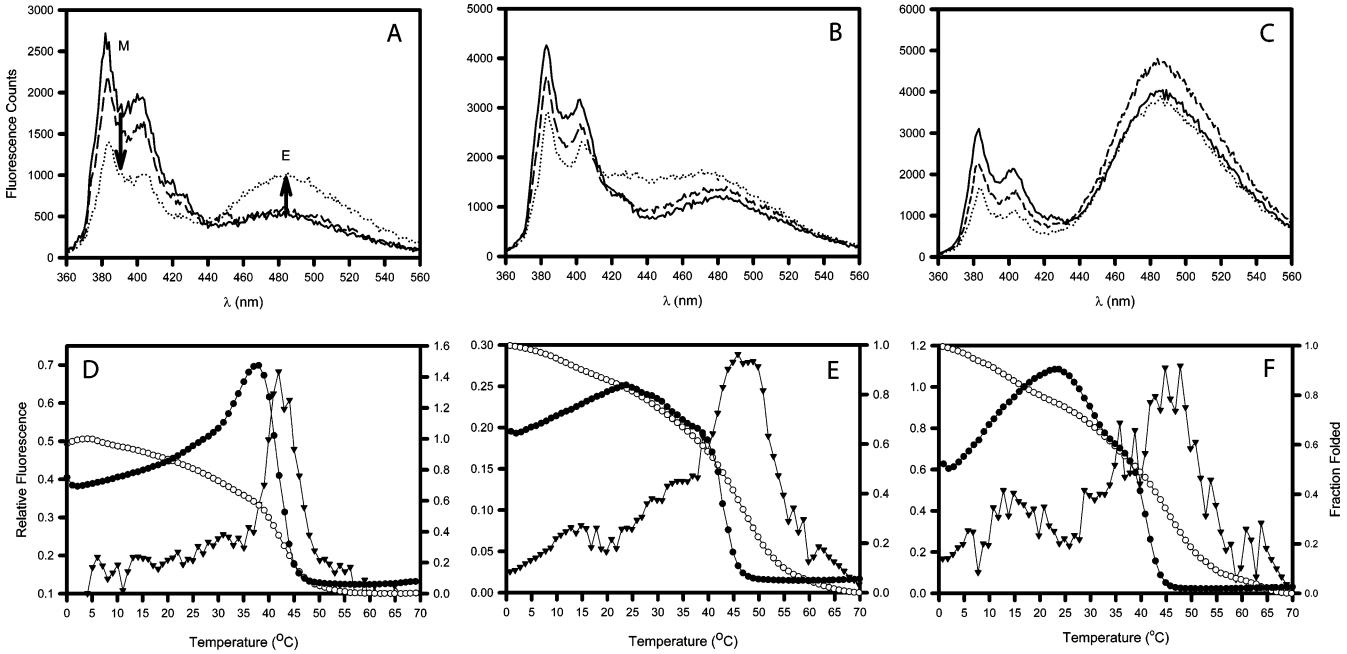

FIGURE 6: Unfolding of tropomyosins labeled at Cys190 with pyrene iodoacetamide to measure the relationship between loss of α-helix and the increase in pyrene excimer fluorescence. The protein concentration was 0.01 mg/mL in 500 mM NaCl, 10 mM sodium phosphate (pH 7.5), 1 mM EDTA, 1 mM DTT. (A, D) Wild-type. (B, E) p1p5. (C, F) p2p5Shift. (A−C) Fluorescence scans at increasing temperatures: 12 °C (solid line), 20 °C (dashed line), and 35 °C (dotted line). All show a rise in excimer with a drop in monomer; however, p2p5Shift has an initially high excimer indicating local flexibility/instability. (D−F) Temperature-dependent unfolding of tropomyosin monitored using circular dichroism and the excimer fluorescence. The final transition of the thermal unfolding, with a loss of ellipticity and fluorescence, accompanies chain dissociation. The increase in pyrene fluorescence occurs during a pretransition, prior to chain dissociation. Symbols: ○, ellipticity; ▼, first derivative of the ellipticity isotherm; ●, excimer fluorescence. The excimer signal is lost for the wild-type and TM mutants prior to main chain unfolding, indicating local flexibility and instability.

Ca^{2+} binding to troponin C (*48*, *49*). The period 1 sequence may be specific for forming the overlap complex with the C-terminus.

Assessment of Stability: Thermal Stability of Mutants Measured Using Circular Dichroism. Circular dichroism (CD) was used to measure the temperature dependence of the unfolding of the α-helical coiled coil. Replacement of the native period 5 sequence by period 1 in p1p5 stabilized the molecule, increasing the temperature of 50% unfolding from 45.0 °C for the wild-type to 48.9 °C (Figure 2B, Table 3). This is surprising because of the Ala cluster and fewer stabilizing residues at the interface than in the wild-type. There were multiple transitions, with the main transition increasing from 46.2 to 51.0 °C but with similar cooperativity of unfolding. The pretransition T_{M1} (34.2 °C) of the wild-type in the region of the mutations is broadened in the p1p5 mutant (Figure 6E).

Replacement of the native period 5 sequence by variations of period 2 gave results consistent with previous work done with period 5 mutations (*14*). The p2p5Shift and p2p5AC mutants destabilized the molecule with lower cooperativity of unfolding and decreased the 50% unfolding to 43.4 and 43.3 °C, respectively, compared to 45.0 °C for the wild-type (Figure 3B, Table 3). The T_M of the main unfolding and pretransition both decreased, from 46.2 and 34.2 °C, respectively, in the wild-type to 43.3 and 32.4 °C in the p2p5AC mutant. In contrast, the p2p5Shift mutant was less cooperative with a broad unfolding transition, without a discernible pretransition. As expected, the p2p5NC mutant stabilized the molecule, increasing the T_M of the major transition, from 46.2 to 54.4 °C, and the 50% unfolding to 47.9 °C. There were multiple transitions, with most of the molecule unfolding with lower cooperativity and at a higher temperature compared to the wild-type. The stabilizing effect of a single interface Leu in a destabilizing cluster (YLA) is consistent with our observed results for periods 1, 2, and 5 and systematic analyses of model peptides containing stabilizing residues in destabilizing clusters (*7*, *13*, *14*, *50*).

Assessment of Stability: Local Stability Measured Using Pyrene Fluorescence. The mutants have predicted global stabilities, except the p1p5 mutant, which is more stable than expected. To determine whether the increased global stability in p1p5 reflects increased local stability in the region of the mutation, we labeled Cys190, proximal to our mutations, with a conformational probe, pyrene iodoacetamide. Analysis of pyrene-labeled tropomyosin has shown that the broad pretransition seen during thermal denaturation corresponds to local unfolding of the Cys190 region that includes residues 165−188 (*33*, *51*, *52*). As tropomyosin unfolds, local side chain flexibility allows for the reorientation of the pyrene monomers from each Cys to form an interacting dimer between the chains, leading to an increase in the excimer fluorescence. Chain separation during the main transition leads to the loss of excimer fluorescence.

The wild-type tropomyosin and p1p5 and p2p5Shift mutants were labeled at Cys190 with PIA, and the fluorescence profile of each was determined at temperatures below and close to the pretransition (Figure 6A−C). Figure 6D shows the characteristic unfolding profile of PIA−wild-type in which the excimer fluorescence increases during the pretransition and is lost during the main transition (46.2 °C) (*33*). The unfolding of both PIA−p1p5 and PIA−p2p5Shift occurred over a broader temperature range and was less cooperative (Figure 6E,F). The pyrene excimer fluorescence

of PIA−p2p5Shift was high relative to monomer fluorescence at low temperatures (Figure 6C) and increased at temperatures well below the main unfolding transition (19.8 vs 42.6 °C), indicating that the mutation destabilized the interface and neighboring regions, as we previously reported with PIA−Exon 5-QNQ (*14*). The excimer fluorescence was lost in both PIA−p1p5 and PIA−p2p5Shift prior to the main unfolding peak, indicating that the Cys190 region, and therefore the mutated regions themselves, is locally destabilized. These results suggest that the increased global stability observed for p1p5 is due to long-range effects, but it is locally destabilized near the Ala cluster region.

DISCUSSION

Our work shows that generic and specific periodic features of the tropomyosin molecule are essential for function. An unstable coiled coil interface and the presence of specific noninterface "consensus" residues are generic requirements. In this regard, the periodic repeats *are* quasi-equivalent for the most basic tropomyosin property, the ability to bind to filamentous actin. On the other hand, the regulatory functions, binding to the actin filament in the strong, force-producing state and Ca^{2+}-dependent regulation with troponin, involve specific regions of the molecule.

The most quasi-equivalent feature for actin binding is the "consensus" residues, seven surface residues distributed with the appropriate 7-fold periodicity to bind actin monomers in the filament (*6*). Even though they are not identical in different periods, they are quasi-interchangeable, as illustrated by the ability of the p1p5 and p2p5AC mutants to bind actin. The failure of p2p5Shift to bind actin shows that proper axial alignment of the consensus residues is essential for actin binding. Other evidence for axial specific interactions between tropomyosin and actin comes from an earlier study of tropomyosin mutants in which deletion of one-third, half, or two-thirds of period 2 (based on a 42-residue repeat) destroyed actin affinity (*19*, *53*). However, in the presence of troponin the half-period deletion mutant bound, lending support to the McLachlan and Stewart proposal of 14 quasi-equivalent sites (*5*) and raising the question of how troponin can moderate and modify the binding between actin and tropomyosin. Even though we have only a short fragment of troponin T in our binding studies that binds far from period 5, we cannot rule out a qualitative influence on actin binding.

The lower actin affinity of the p1p5 and p2p5AC mutants (the present study) and the Exon 5-Zip-Revert mutant (*14*), compared to the wild-type, indicates that features beyond the consensus residues and destabilizing clusters contribute to actin−tropomyosin interactions. Periods 1 and 2 may be specialized for their own site-specific functions, such as formation of the overlap complex in the case of period 1 (*11*, *25*, *38*). Alternatively, the lower affinity of the mutants may result from unfavorable interactions introduced by the mutant sequences.

Successful replacement of period 5, which contains an Ala cluster, with another period depends on an unstable interface. The effects are subtle. Replacement of the noncanonical, destabilizing period 2 YLA interface in p2p5NC with AAS in p2p5AC decreases the overall T_M by 6 °C and increases the actin affinity by 50%. The results are consistent with modeling and experimental work which show that the stability of tropomyosin is related to the hydrophobicity and packing of the core (*13*, *32*). In p2p5NC, Leu improves core packing with respect to the flanking Tyr and Ala. The YLA interface, while more stable than AAS, is much less stable than a canonical coiled coil interface, such as LVL, which results in loss of actin binding when substituted for either the period 2 or the period 5 Ala cluster (*13*, *14*). In structural studies, the side chains of Tyr and Gln at the a and d positions, respectively, are more dynamic than canonical interface residues (*11*, *15*). We suggest that the destabilizing effect of the Ala clusters in the core of the molecule allows the mobility of noninterface tropomyosin side chains to optimize binding to sites on actin and confers the flexibility required for the coiled coil to assume the helical parameters of the actin filament. Furthermore, the weaker binding of tropomyosin to filamentous actin at low temperatures (*54*) may be a consequence of a more fully folded, less dynamic coiled coil that is optimized for function at physiological temperatures.

In their original analysis of striated muscle α-tropomyosin, McLachlan et al. noted that period 1 is the most similar to period 5. The two periods have consistent and parallel deviations from the other periods (*42*). We suggest this is not a coincidence and that periods 1 and 5 are specialized for maximal binding affinity; these are the only periods with Ala clusters embedded within the consensus repeats (Figure 1). Period 1, at one end of the molecule, and period 5, in the middle, provide two "strong" binding sites that give the molecule an optimal level of affinity necessary for the dynamic movement of tropomyosin on the actin filament between the blocked state with troponin in the absence of Ca^{2+} and the open state in the presence of Ca^{2+} and strong-binding myosin cross-bridges.

The regulatory functions of tropomyosin occur on the actin filament; therefore, the consensus residues are, de facto, required. However, the consensus repeats are not quasi-equivalent in their regulatory functions. The similar period 1 and period 5 repeats are comparable in their ability to interact with actin in the strong, force-producing state with myosin, whereas the period 2 consensus repeat is not, even with an Ala cluster. The specificity of the surface consensus residues is illustrated by near full recovery of function when they were introduced into the destabilized Exon 5-Zip mutants in "Exon 5-Zip-Revert" that had near normal myosin S1-promoted binding and regulation of the actomyosin ATPase with troponin. The present results underline the importance of the midregion of tropomyosin, including periods 3−5 for myosin to shift the thin filament to the open state, as previously documented in studies of deletion and substitution mutants (*17*, *18*, *55*−*58*). Most of this region is contained between two global bends in the tropomyosin molecule (*12*). Periods 3−5 are encoded by constitutively expressed exons and are present in all muscle and nonmuscle tropomyosins encoded by the α-tropomyosin gene (TPM1), implicating their involvement in conserved functions.

In addition to its role in activation of the actin filament, period 5 is specialized for troponin-dependent regulation. Since inhibition of actin−myosin interaction by p1p5 in the absence of Ca^{2+} is poor, we conclude that the period 1 consensus region cannot substitute for period 5 for this function. Just as the C-terminal region of tropomyosin encoded by exon 9 is specialized for binding troponin T (*34*,

59−*61*), periods 5 and 6 are designed for regulatory function with troponin (this work, *62*), even though they are expressed in cells that do not have troponin (*3*).

In summary, we show in the present work that generic and specific features of the tropomyosin molecule have roles in actin binding. The results give experimental support for previous proposals (*5*, *7*, *8*) and emphasize that interface instability is critical for providing local flexibility that allows tropomyosin to wind around the helical actin filament. In addition, the results emphasize the importance of the midregion of the tropomyosin molecule for its regulatory functions.

ACKNOWLEDGMENT

We thank Dr. Norma Greenfield for many discussions and Ms. Lucy Kotylanskaya for assistance in protein preparation. This work was carried out in partial fulfillment of the Ph.D. degree from the Graduate Program in Biochemistry and Molecular Biology (*63*).

REFERENCES

1. Perry, S. V. (2001) Vertebrate tropomyosin: distribution, properties and function, *J. Muscle Res. Cell Motil. 22*, 5−49.
2. Brown, J. H., and Cohen, C. (2005) Regulation of muscle contraction by tropomyosin and troponin: how structure illuminates function, *Adv. Protein Chem. 71*, 121−159.
3. Gunning, P. W., Schevzov, G., Kee, A. J., and Hardeman, E. C. (2005) Tropomyosin isoforms: divining rods for actin cytoskeleton function, *Trends Cell Biol. 15*, 333−341.
4. Parry, D. A., and Squire, J. M. (1973) Structural role of tropomyosin in muscle regulation: analysis of the x-ray diffraction patterns from relaxed and contracting muscles, *J. Mol. Biol. 75*, 33−55.
5. McLachlan, A. D., and Stewart, M. (1976) The 14-fold periodicity in alpha-tropomyosin and the interaction with actin, *J. Mol. Biol. 103*, 271−298.
6. Phillips, G. N., Jr. (1986) Construction of an atomic model for tropomyosin and implications for interactions with actin, *J. Mol. Biol. 192*, 128−131.
7. Kwok, S. C., and Hodges, R. S. (2004) Stabilizing and destabilizing clusters in the hydrophobic core of long two-stranded alpha-helical coiled-coils, *J. Biol. Chem. 279*, 21576−21588.
8. Brown, J. H., Kim, K. H., Jun, G., Greenfield, N. J., Dominguez, R., Volkmann, N., Hitchcock-DeGregori, S. E., and Cohen, C. (2001) Deciphering the design of the tropomyosin molecule, *Proc. Natl. Acad. Sci. U.S.A. 98*, 8496−8501.
9. Li, Y., Mui, S., Brown, J. H., Strand, J., Reshetnikova, L., Tobacman, L. S., and Cohen, C. (2002) The crystal structure of the C-terminal fragment of striated-muscle alpha-tropomyosin reveals a key troponin T recognition site, *Proc. Natl. Acad. Sci. U.S.A. 99*, 7378−7383.
10. Brown, J. H., Zhou, Z., Reshetnikova, L., Robinson, H., Yammani, R. D., Tobacman, L. S., and Cohen, C. (2005) Structure of the mid-region of tropomyosin: bending and binding sites for actin, *Proc. Natl. Acad. Sci. U.S.A. 102*, 18878−18883.
11. Greenfield, N. J., Huang, Y. J., Swapna, G. V., Bhattacharya, A., Rapp, B., Singh, A., Montelione, G. T., and Hitchcock-Degregori, S. E. (2006) Solution NMR structure of the junction between tropomyosin molecules: Implications for actin binding and regulation, *J. Mol. Biol. 364*, 80−96.
12. Nitanai, Y., Minakata, S., Maeda, K., Oda, N., and Maeda, Y. (2007) Crystal structures of tropomyosin: flexible coiled-coil, *Adv. Exp. Med. Biol. 592*, 137−151.
13. Singh, A., and Hitchcock-DeGregori, S. E. (2003) Local destabilization of the tropomyosin coiled coil gives the molecular flexibility required for actin binding, *Biochemistry 42*, 14114−14121.
14. Singh, A., and Hitchcock-DeGregori, S. E. (2006) Dual requirement for flexibility and specificity for binding of the coiled-coil tropomyosin to its target, actin, *Structure 14*, 43−50.
15. Greenfield, N. J., Swapna, G. V., Huang, Y., Palm, T., Graboski, S., Montelione, G. T., and Hitchcock-DeGregori, S. E. (2003) The structure of the carboxyl terminus of striated alpha-tropomyosin in solution reveals an unusual parallel arrangement of interacting alpha-helices, *Biochemistry 42*, 614−619.
16. Dyson, H. J., and Wright, P. E. (2005) Intrinsically unstructured proteins and their functions, *Nat. Rev. Mol. Cell Biol. 6*, 197−208.
17. Hitchcock-DeGregori, S. E., Song, Y., and Moraczewska, J. (2001) Importance of internal regions and the overall length of tropomyosin for actin binding and regulatory function, *Biochemistry 40*, 2104−2112.
18. Hitchcock-DeGregori, S. E., Song, Y., and Greenfield, N. J. (2002) Functions of tropomyosin's periodic repeats, *Biochemistry 41*, 15036−15044.
19. Hitchcock-DeGregori, S. E., and An, Y. (1996) Integral repeats and a continuous coiled coil are required for binding of striated muscle tropomyosin to the regulated actin filament, *J. Biol. Chem. 271*, 3600−3603.
20. Ruiz-Opazo, N., and Nadal-Ginard, B. (1987) Alpha-tropomyosin gene organization. Alternative splicing of duplicated isotype-specific exons accounts for the production of smooth and striated muscle isoforms, *J. Biol. Chem. 262*, 4755−4765.
21. Studier, F. W., Rosenberg, A. H., Dunn, J. J., and Dubendorff, J. W. (1990) Use of T7 RNA polymerase to direct expression of cloned genes, *Methods Enzymol. 185*, 60−89.
22. Wang, W., and Malcolm, B. A. (1999) Two-stage PCR protocol allowing introduction of multiple mutations, deletions and insertions using QuikChange Site-Directed Mutagenesis, *Biotechniques 26*, 680−682.
23. Studier, F. W. (2005) Protein production by auto-induction in high density shaking cultures, *Protein Expr. Purif. 41*, 207−234.
24. Hitchcock-DeGregori, S. E., and Heald, R. W. (1987) Altered actin and troponin binding of amino-terminal variants of chicken striated muscle alpha-tropomyosin expressed in Escherichia coli, *J. Biol. Chem. 262*, 9730−9735.
25. Cho, Y. J., Liu, J., and Hitchcock-DeGregori, S. E. (1990) The amino terminus of muscle tropomyosin is a major determinant for function, *J. Biol. Chem. 265*, 538−545.
26. Hitchcock-DeGregori, S. E., Mandala, S., and Sachs, G. A. (1982) Changes in actin lysine reactivities during polymerization detected using a competitive labeling method, *J. Biol. Chem. 257*, 12573−12580.
27. Potter, J. D. (1982) Preparation of troponin and its subunits, *Methods Enzymol. 85*, 241−263.
28. Palm, T., Graboski, S., Hitchcock-DeGregori, S. E., and Greenfield, N. J. (2001) Disease-causing mutations in cardiac troponin T: identification of a critical tropomyosin-binding region, *Biophys. J. 81*, 2827−2837.
29. Edelhoch, H. (1967) Spectroscopic determination of tryptophan and tyrosine in proteins, *Biochemistry 6*, 1948−1954.
30. Lehrer, S. S. (1975) Intramolecular crosslinking of tropomyosin via disulfide bond formation: evidence for chain register, *Proc. Natl. Acad. Sci. U.S.A. 72*, 3377−3381.
31. Fasman, G. D. (1989) *Practical Handbook of Biochemistry and Molecular Biology*, CRC Press, Boca Raton, FL.
32. Greenfield, N. J., and Hitchcock-DeGregori, S. E. (1995) The stability of tropomyosin, a two-stranded coiled-coil protein, is primarily a function of the hydrophobicity of residues at the helix-helix interface, *Biochemistry 34*, 16797−16805.
33. Ishii, Y., and Lehrer, S. S. (1990) Excimer fluorescence of pyrenyliodoacetamide-labeled tropomyosin: a probe of the state of tropomyosin in reconstituted muscle thin filaments, *Biochemistry 29*, 1160−1166.
34. Hammell, R. L., and Hitchcock-DeGregori, S. E. (1996) Mapping the functional domains within the carboxyl terminus of alpha-tropomyosin encoded by the alternatively spliced ninth exon, *J. Biol. Chem. 271*, 4236−4242.
35. Laemmli, U. K. (1970) Cleavage of structural proteins during the assembly of the head of bacteriophage T4, *Nature 227*, 680−685.
36. White, H. D. (1982) Special instrumentation and techniques for kinetic studies of contractile systems, *Methods Enzymol. 85*, 698−708.
37. Eaton, B. L. (1976) Tropomyosin binding to F-actin induced by myosin heads, *Science 192*, 1337−1339.
38. Moraczewska, J., Nicholson-Flynn, K., and Hitchcock-DeGregori, S. E. (1999) The ends of tropomyosin are major determinants of actin affinity and myosin subfragment 1-induced binding to F-actin in the open state, *Biochemistry 38*, 15885−15892.

39. Whitby, F. G., and Phillips, G. N., Jr. (2000) Crystal structure of tropomyosin at 7 Angstroms resolution, *Proteins 38*, 49−59.
40. Pettersen, E. F., Goddard, T. D., Huang, C. C., Couch, G. S., Greenblatt, D. M., Meng, E. C., and Ferrin, T. E. (2004) UCSF Chimera−a visualization system for exploratory research and analysis, *J. Comput. Chem. 25*, 1605−1612.
41. Phillips, G. N., Jr., Fillers, J. P., and Cohen, C. (1986) Tropomyosin crystal structure and muscle regulation, *J. Mol. Biol. 192*, 111−131.
42. McLachlan, A. D., Stewart, M., and Smillie, L. B. (1975) Sequence repeats in alpha-tropomyosin, *J. Mol. Biol. 98*, 281−291.
43. McKillop, D. F., and Geeves, M. A. (1993) Regulation of the interaction between actin and myosin subfragment 1: evidence for three states of the thin filament, *Biophys. J. 65*, 693−701.
44. Lehrer, S. S., and Geeves, M. A. (1998) The muscle thin filament as a classical cooperative/allosteric regulatory system, *J. Mol. Biol. 277*, 1081−1089; erratum, *J. Mol. Biol. 279* (4), 1024.
45. Geeves, M. A., and Lehrer, S. S. (1994) Dynamics of the muscle thin filament regulatory switch: the size of the cooperative unit, *Biophys. J. 67*, 273−282.
46. Cassell, M., and Tobacman, L. S. (1996) Opposite effects of myosin subfragment 1 on binding of cardiac troponin and tropomyosin to the thin filament, *J. Biol. Chem. 271*, 12867−12872.
47. Moraczewska, J., Wawro, B., Seguro, K., and Strzelecka-Golaszewska, H. (1999) Divalent cation-, nucleotide-, and polymerization-dependent changes in the conformation of subdomain 2 of actin, *Biophys. J. 77*, 373−385.
48. Ishii, Y., and Lehrer, S. S. (1991) Two-site attachment of troponin to pyrene-labeled tropomyosin, *J. Biol. Chem. 266*, 6894−6903.
49. Maytum, R., Lehrer, S. S., and Geeves, M. A. (1999) Cooperativity and switching within the three-state model of muscle regulation, *Biochemistry 38*, 1102−1110.
50. Kwok, S. C., and Hodges, R. S. (2003) Clustering of large hydrophobes in the hydrophobic core of two-stranded alpha-helical coiled-coils controls protein folding and stability, *J. Biol. Chem. 278*, 35248−35254.
51. Betcher-Lange, S. L., and Lehrer, S. S. (1978) Pyrene excimer fluorescence in rabbit skeletal alphaalphatropomyosin labeled with N-(1-pyrene)maleimide. A probe of sulfhydryl proximity and local chain separation, *J. Biol. Chem. 253*, 3757−3760.
52. Graceffa, P., and Lehrer, S. S. (1980) The excimer fluorescence of pyrene-labeled tropomyosin. A probe of conformational dynamics, *J. Biol. Chem. 255*, 11296−11300.
53. Hitchcock-DeGregori, S. E., and Varnell, T. A. (1990) Tropomyosin has discrete actin-binding sites with sevenfold and fourteenfold periodicities, *J. Mol. Biol. 214*, 885−896.
54. Drabikowski, W. a. G. J. (1962) The effect of the temperature of extraction on the tropomyosin content in actin, *J. Biol. Chem. 237*, 3412−3417.
55. Landis, C. A., Bobkova, A., Homsher, E., and Tobacman, L. S. (1997) The active state of the thin filament is destabilized by an internal deletion in tropomyosin, *J. Biol. Chem. 272*, 14051−14056.
56. Landis, C., Back, N., Homsher, E., and Tobacman, L. S. (1999) Effects of tropomyosin internal deletions on thin filament function, *J. Biol. Chem. 274*, 31279−31285.
57. Tobacman, L. S., and Butters, C. A. (2000) A new model of cooperative myosin-thin filament binding, *J. Biol. Chem. 275*, 27587−27593 (in process citation).
58. Sakuma, A., Kimura-Sakiyama, C., Onoue, A., Shitaka, Y., Kusakabe, T., and Miki, M. (2006) The second half of the fourth period of tropomyosin is a key region for Ca(2+)-dependent regulation of striated muscle thin filaments, *Biochemistry 45*, 9550−9558.
59. Cho, Y. J., and Hitchcock-DeGregori, S. E. (1991) Relationship between alternatively spliced exons and functional domains in tropomyosin, *Proc. Natl. Acad. Sci. U.S.A. 88*, 10153−10157.
60. Hammell, R. L., and Hitchcock-DeGregori, S. E. (1997) The sequence of the alternatively spliced sixth exon of alpha- tropomyosin is critical for cooperative actin binding but not for interaction with troponin, *J. Biol. Chem. 272*, 22409−22416.
61. Palm, T., Greenfield, N. J., and Hitchcock-DeGregori, S. E. (2003) Tropomyosin ends determine the stability and functionality of overlap and troponin T complexes, *Biophys. J. 84*, 3181−3189.
62. Maytum, R., Bathe, F., Konrad, M., and Geeves, M. A. (2004) Tropomyosin exon 6b is troponin-specific and required for correct acto-myosin regulation, *J. Biol. Chem. 279*, 18203−18209.
63. Singh, A. (2007) *Biochemistry and Molecular Biology*, p 205, University of Medicine and Dentistry of New Jersey and Rutgers University, Piscataway, NJ.

BI701570B